BIOCHEMISTRY
including biophysical chemistry & molecular biology

Article

pubs.acs.org/biochemistry

Free Energy Study of the Catalytic Mechanism of *Trypanosoma cruzi trans*-Sialidase. From the Michaelis Complex to the Covalent Intermediate

Gustavo Pierdominici-Sottile,[†,‡] Nicole A. Horenstein,[‡] and Adrian E. Roitberg*[,‡,§]

[†]Centro de Estudios e Investigaciones, Universidad Nacional de Quilmes, Sáenz Peña 352, B1876BXD Bernal, Argentina

[‡]Department of Chemistry, University of Florida, Gainesville, Florida 32611-8435, United States

[§]Quantum Theory Project, University of Florida, Gainesville, Florida 32611-8435, United States

ABSTRACT: *Trypanosoma cruzi trans*-sialidase (TcTS) is a crucial enzyme for the infection of *Trypanosoma cruzi*, the protozoa responsible for Chagas' disease in humans. It catalyzes the transfer of sialic acids from the host's glycoconjugates to the parasite's glycoconjugates. Based on kinetic isotope effect (KIE) studies, a strong nucleophilic participation at the transition state could be determined, and recently, elaborate experiments used 2-deoxy-2,3-difluorosialic acid as substrate and were able to trap a long-lived covalent intermediate (CI) during the catalytic mechanism. In this paper, we compute the KIE and address the entire mechanistic pathway of the CI formation step in TcTS using computational tools. Particularly, the free energy results indicate that in the transition state there is a strong nucleophilic participation of Tyr342, and after this, the system collapsed into a stable CI. We find that there is no carbocation intermediate for this reaction. By means of the energy decomposition method, we identify the residues that have the biggest influence on catalysis. This study facilitates the understanding of the catalytic mechanism of TcTS and can serve as a guide for future inhibitor design studies.

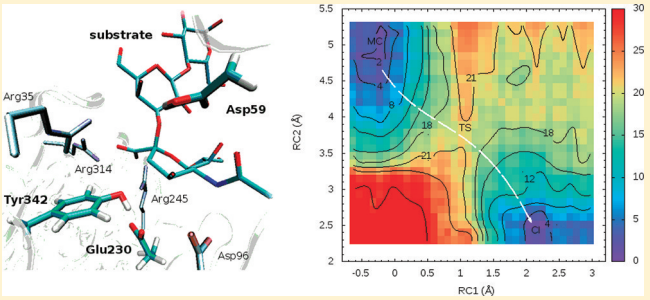

Chagas disease (American trypanosomiasis) is a lethal, chronic disease of humans and other mammals. It is widely found in Central and South America with 17 million people currently infected according to World Health Organization's estimates. It has a death toll of 50 000 people each year.[1] Chagas disease is caused by the protozoan parasite *Trypanosoma cruzi*, and no effective drug or vaccine exists although it has been a century since the disease was discovered.

T. cruzi's infectivity in the human body depends on the enzyme *trans*-sialidase (TcTS).[2−6] Unable to synthesize sialic acid,[7] which is used for human cell recognition,[8,9] *T. cruzi* would be vulnerable in the host body.[4,5] However, sialic acids transferred to its surface glycoconjugates by TcTS provide *T. cruzi* the ability to evade the immune system of the host and to adhere to and invade the host cells.[10] The parasite invasion is found to be significantly reduced when sialylated epitopes are neutralized with antibodies,[11] when TcTS is neutralized by various other protocols[12−14] or when sialic acids are present in neither the host cells nor the external medium.[10] The direct involvement of this enzyme in animal pathogenesis[15] and thymocyte apoptosis[16] has also been shown. The genome of *T. cruzi* is found to have many copies of the genes encoding for TcTS and its isoforms (constituting ∼15% of the entire genome).[17] Having such an important role in Chagas disease infection, TcTS has been the focus of many studies. The lack of this enzyme or analogues in humans presents the enzyme as a potential and appealing therapeutic target for the disease.

TcTS catalyzes the transfer of α-(2→3) sialic acid from sialoglycoconjugates to β-galactosyl glycoconjugates, with retention of configuration.[3] TcTS is a member of the CAZY GH33[18] family,[19] which is part of the superfamily of sialidase enzymes. This family features a 6-fold β-propeller structure, and members feature an active site tyrosine residue as the putative nucleophile. An overview of various GH33 mechanisms has been reported.[20] Interestingly, TcTS is unlike most family members, in that TcTS is not a committed hydrolase. It acts through a ping-pong mechanism (i.e., double displacement mechanism) in which binding of the first substrate leads to a modified enzyme form with the sugar glycon, which then binds to the second acceptor substrate and forms the final product.[21−23] In the initial stages of the mechanism, the sialic acid is scavenged from the donor glycoconjugate with evidence suggesting nucleophilic participation of the enzyme at the transition state.[24] A historical question for glycosidases is whether there is nucleophilic participation, requiring collapse into a covalent intermediate (CI), or if the bound substrate remains as an oxocarbenium ion. This has been long discussed for enzymes of similar families, even for the very well-studied lysozyme.[25−28] In the case of sialic acids, the question is

Received: June 23, 2011
Revised: September 21, 2011
Published: October 18, 2011

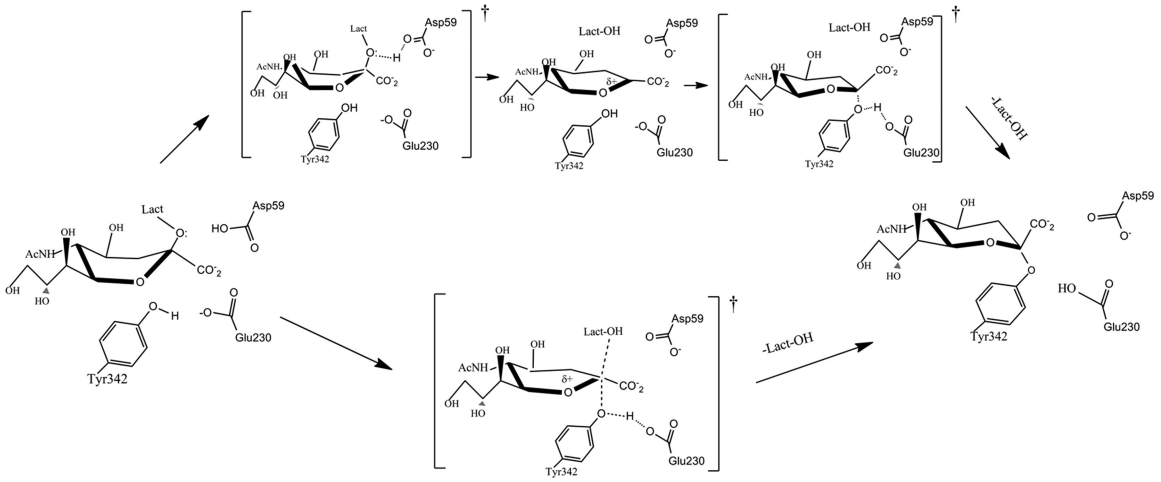

Figure 1. Two possible paths (considering or not an oxocarbenium intermediate) to reach the covalent intermediate in the catalytic mechanism of TcTS.

especially interesting given the somewhat enhanced stability its oxocarbenium ion has in solution, relative to conventional sugars such as glucose.[29]

For TcTS-catalyzed reaction of sialic acid glycosides, kinetic isotope effect (KIE) studies revealed strong nucleophilic participation in the transition state (TS), and these results together with the fact that this enzyme retains the stereochemistry around the reaction center pointed toward subsequent CI formation.[30] In a separate effort, the TcTS CI was trapped, and Tyr342 was identified—unprecedented among retaining glycosidases[31]—as the nucleophile that attack the anomeric C atom of the sialic acid.[23] The identification of a tyrosine acting as a nucleophile for TcTS catalysis was first deemed unlikely[31] because glycosidases (e.g., lysozyme) usually use a pair of protein carboxylates (Asp or Glu residues) as the nucleophile and the acid/base catalyst.[32,33] It was suggested that as both the sialic acid and a Glu (or Asp) residue possess a carboxylate group, a carboxylate residue acting as a direct nucleophile would generate unfavorable interactions. However, by using a Tyr/Glu couple, TcTS would achieve appreciable negative character on the phenolic oxygen only at the TS.[23] This change in the nucleophilic character of Tyr342 after the proton transfer to Glu230, which is enhanced upon substrate binding, has been recently examined by us.[34]

In the rest of the article we will use the IUPAC nomenclature for substitution transformation[35] where the reactions are written in terms of associative (A) and dissociative (D) processes. Thus, a concerted bimolecular "S_N2" displacement will be written as A_ND_N. $D_N + A_N$ and $D_N{}^*A_{Nint}$ denote stepwise "S_N1" mechanisms. The "+" symbol indicates that the intermediate carbocation can diffuse away before it reaches the nucleophilic reagent, while "∗" represents a short-living intermediate formed faster than diffusing away. A_ND_N reactions may also be divided into dissociative or associative classifications depending on the relation between the nucleophilic approach and the departure of the leaving group. An A_ND_N (dissociative) mechanism indicates that in the TS the loss of bonding has progressed further than bond formation. When these characteristics are inverted, the mechanism is considered associative.

The detailed way in which the CI is reached in the mechanism of TcTS is still being investigated. In Figure 1, the two extreme cases for reaching the CI from the Michaelis complex in TcTS are depicted. Traditional physical organic chemistry arguments would suggest that the formation could not happen through an A_ND_N mechanism due to the highly hindered reaction site, arguing for a dissociative path with little or no nucleophilic participation from Tyr342 (upper path in Figure 1). However, the architecture of the active site can plausibly change the mechanism to an A_ND_N route where bond breaking and making are concerted to some degree (lower path in Figure 1). In this article, we investigate the conversion from the Michaelis complex (MC) to the CI in the mechanism of TcTS with sialyllactose using the umbrella sampling technique. The stabilization pattern of the active site residues on the transition state (TS) in relation to the MC is examined by means of the energy decomposition method. KIE calculations considering a model of the enzyme active site are also depicted.

The rest of the article is organized as follows. In the next section we briefly describe the methodologies employed in the calculations. Then, we present the results and discuss them. Finally, the conclusions of this work are outlined.

METHODS

General Aspects. The crystal structure of TcTS in complex with sialyllactose was used as the starting geometry (PDB entry code 1S0I[21]). In what follows, the numbers of residues and the names of the atoms correspond to this crystallographic structure. Asp59 acts as an acid/base catalyst during the enzyme mechanism, so it was experimentally mutated to Ala59 prior to crystallization to protect the ligand from hydrolysis.[31] In our simulations, in order to model the wild-type form, Ala59 was mutated *in silico* back to Asp59. The resulting structure was fed into the leap module of the AMBER10 molecular dynamics package[36] where the necessary hydrogen atoms were added. The system was solvated in a truncated octahedral cell of TIP3P[37] explicit water molecules. The ff99SB[38,39] force field was used to construct the topology files. In all quantum mechanics/molecular mechanics (QM/MM) simulations, the self-consistent charge density functional tight binding (scc-DFTB),[40] as implemented in AMBER10,[41] was the level of theory selected to describe the potential energy of the QM subsystem. The particle mesh Ewald method was used to calculate the long-range Coulomb force. The initial structure was minimized at constant volume, and in a second stage, the system was heated, at constant volume, from 0 K to a

dx.doi.org/10.1021/bi2009618|*Biochemistry* 2011, 50, 10150–10158

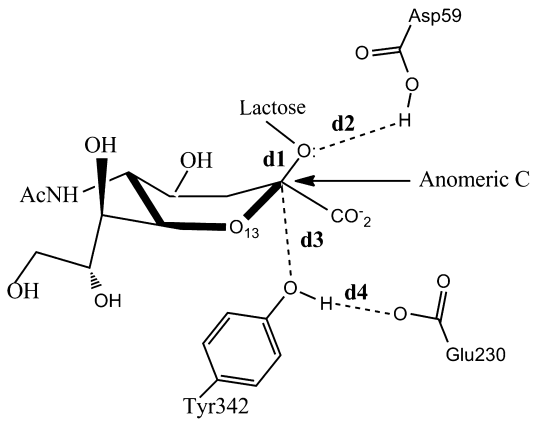

Figure 2. Distances used to scan the 2-D reaction coordinate. *d*1 refers to the distance between the anomeric C atom of sialic acid and the glycosidic O of lactose. *d*2 is the distance between the glucosidic O of lactose and the H atom of the carboxylic group of Asp59, *d*3 is the one between the anomeric C of the sialic acid and the hydroxyl O atom of Tyr342, and *d*4 describes that which involves one carboxyl O atom of Glu230 and the hydroxyl H atom of Tyr342.

target temperature of 300 K during 55.0 ps using the weak-coupling algorithm with a τ_{tp} value of 2.8 ps. After this, we switched to constant temperature and pressure conditions, using a value of 2.0 ps for both τ_{tp} and τ_p. Finally, a 300 ps molecular dynamics (MD) simulation was practiced in order to equilibrate the system. This MD simulation, as well as all the others carried out in this work, was performed using periodic boundary conditions with a cutoff distance of 12.0 Å and a time step of 1.0 fs. The equilibrated structure was used as the initial point for the umbrella sampling analysis.

Umbrella Sampling Calculations. The distances involved in the reaction coordinate definitions are depicted in Figure 2: *d*1 refers to the distance between the anomeric C atom of sialic acid and the glycosidic O of lactose, and *d*2 accounts for that between the glycosidic O of lactose and the H atom of the carboxylic group of Asp59. *d*3 defines the distance between the anomeric C of the sialic acid and the hydroxyl O atom of Tyr342 while *d*4 describes the distance between one carboxyl O atom of Glu230 and the hydroxyl H atom of Tyr342. A 2-D free energy profile was evaluated to explore the formation of the CI in the mechanism of TcTS, defining two coordinates: RC1 = *d*1 − *d*2 and RC2 = *d*3 + *d*4. RC1 was sampled from −0.61 to 2.91 Å while RC2 was scanned from 5.24 to 2.36 Å. The scans were done in steps of 0.08 Å. In each point of the grid, a 25 ps QM/MM MD simulation was performed constraining the value of the 2-D reaction coordinate with a harmonic potential using a force constant of 450.0 kcal/mol. The last structure of an umbrella window run was used as the starting point for the next one. Structures and the value for the reaction coordinate were dumped every 200 and 2.0 fs, respectively. Before each production MD run, a 10 ps equilibration phase was carried out. The 2-D weighted histogram analysis method (WHAM-2D)[42] implemented in the package written by Alan Grossfield was used to analyze the probability density and to obtain the free energy profiles for the unbiased system along the reaction coordinate. Statistical uncertainties for each point were calculated with a Monte Carlo bootstrap error analysis[43] as implemented within the WHAM program. To evaluate if the free energy results were time converged, we scanned RC1 from −0.61 to 2.91 Å fixing RC2 equal to 5.0. Another 1-D sampling was carried out fixing RC1 equal to 2.5 and scanning RC2 from 5.24 to 2.36 Å. These two 1-D analyses were done in exactly the same conditions as those for the 2-D examination except that each MD simulation lasted 50 ps.

Interaction Energy Decomposition. We used the energy decomposition method to analyze how the active site residues stabilize/destabilize the TS in the catalyzed reaction of TcTS with sialyllactose. This method has been extensively applied to enzymes[44−51] and was recently employed by us to understand how the presence of the substrate modifies the ΔG_r^0 for the proton transfer from Tyr342 to Glu230 in the catalytic mechanism of this reaction.[34] The influence of an individual residue on the energy of a particular structure is measured taking into account the difference of energies when a particular residue is present (denoted by *i* in eq 1) or when it is replaced by Gly (*i* − 1 in eq 1)[50,51]

$$\Delta E_i = [E_i^{QM} + E_i^{QMMM}] - [E_{i-1}^{QM} + E_{i-1}^{QMMM}] \quad (1)$$

where each term in brackets represents the energy of the QM subsystem influenced by the classical environment. Then, the differences between the stabilization effects in going from MC to TS, for each residue, were estimated by

$$\Delta\Delta E_i = \Delta E_i^{TS} - \Delta E_i^{MC} \quad (2)$$

In the present analysis, the QM subsystem was composed by the substrate and Asp59. To calculate the average values for the interaction energy and stabilization effects ($\langle\Delta\Delta E_i\rangle$) of each residue in a particular configuration, 125 snapshots from MD simulations were considered taken from the umbrella sampling calculation with reaction coordinates corresponding to the MC and TS. The method was applied for residues in which the distance between their center of mass and the center of mass of the QM subsystem was <10.0 Å in the crystallographic structure. This includes 75 residues for the active site of TcTS.

DFTB Validation. Full QM calculations were performed in order to validate the semiempirical level of theory implemented in QMMM calculations. For this purpose, we used a model system containing residues Asp59, Tyr342, Glu230, and sialyllactose. To construct this model, we started from the crystallographic structure of the enzyme, cut the bonds linking the Cα atoms to the rest of the protein backbone, and then filled the free valence of each Cα with hydrogen atoms. From the one side and using the Sander module implemented in AMBER10, we scanned the DFTB minimum energy path (MEP) sampling RC1 vs RC2 considering the same conditions as the one mentioned for the umbrella sampling study. During these computations, the Cα atoms of the three residues of the model were fixed at their initial positions so as to mimic the distances in the protein environment. By the other side and using the GAUSSIAN09[52] program, optimizations for reactants (MC like-configurations), transition states, and products (CI like-configurations) were performed using Hartree−Fock (HF) and density functional theory (with a B3LYP functional). The initial structures employed were taken from the DFTB MEP surface, and the same kind of restraints was also applied for these computations. MP2 methodology was also employed to perform single point calculation on the structures minimized at the DFTB level of theory. The basis set 6-31G(d) was implemented for HF, B3LYP, and MP2 calculations.

KIE Calculations. Two distinct systems were taken into account for these computations. One of them was the one mentioned above for the DFTB validation composed by Asp59,

Tyr342, Glu230, and sialyllactose. The other system consisted in sialyllactose and H_3O^+ and was considered in order to investigate the KIE for the $A_N + D_N$ acid solvolysis of sialyllactose. For both systems, the reactants and TS structure were obtained by means of the B3LYP/6-31G(d) methodology, and the frequencies were computed at the same level of theory. These calculations were performed using GAUSSIAN09.[52] For the sialyllactose acid solvolysis case, water was modeled as an implicit solvent, and the polarizable continuum model[53] was implemented for this fact.

Frequencies results were employed to estimate the KIEs at 299 K considering eq 3[54]

$$\mathrm{KIE} = \frac{k_L}{k_H} = \frac{\nu_L^{\#}}{\nu_H^{\#}} \prod_i^{3n^R-6} \frac{\mu_{iH}^R}{\mu_{iL}^R} \frac{\sinh(\mu_{iL}^R/2)}{\sinh(\mu_{iH}^R/2)} \prod_i^{3n^{\#}-7} \frac{\mu_{iL}^{\#}}{\mu_{iH}^{\#}} \frac{\sinh(\mu_{iH}^{\#}/2)}{\sinh(\mu_{iL}^{\#}/2)} \quad (3)$$

where L and H denote the light and heavy isotopes, respectively. R denotes reactants while the symbol "#" does it for the transition state; n is the number of atoms, ν are the frequencies, and $\nu^{\#}$, particularly, is the imaginary frequency of crossing the barrier. μ is equal to $h\nu/kT$, where T is the temperature and h and k are Planck's and Boltzmann's constants, respectively. These calculations were performed by means of the Isoeff98 program.[55]

RESULTS AND DISCUSSION

The DFTB method not only has been shown to be an accurate level of theory for describing the energetics of chemical reactions,[56] but it was also demonstrated for biological systems that MEP results are also in good agreement with higher levels of theory like MP2.[57] Recently, it was also shown that DFTB provides the best semiempirical description of six-membered carbohydrate ring deformation.[58] For the model system containing Asp59, Tyr342, Glu230, and sialyllactose, rmsd results of the minimized reactants and products structures obtained with DFTB, HF, and B3LYP are similar, indicating that the geometries are being well reproduced by the semiempirical method. Nevertheless, although, DFTB and B3LYP ΔEs are close each other (difference <3.0 kcal/mol), HF produces a significant overestimation of this value (see Table 1). Regarding the barriers, DFTB and HF results overestimate the B3LYP values. However, it should be remarked that, although the MP2 level of theory was implemented for single point calculations of DFTB optimized structures, this semiempirical methodology closely mimics its ΔE and $\Delta E^{\#}$, indicating that DFTB reproduce suitably MP2 barriers and energy changes.

Table 1. Comparison of the ΔE, $\Delta E^{\#}$, and Root-Mean-Square Deviations between the Different Levels of Theory Used To Study the Model System Which Includes Asp59, Glu230, Tyr342, and the Substrate

parameter	DFTB	Hartree−Fock	B3LYP	MP2
reactants rmsd (Å)		0.26	0.20	
products rmsd (Å)		0.19	0.18	
ΔE (kcal/mol)	−0.62	12.11	2.32	0.88
$\Delta E^{\#}$ (kcal/mol)	30.43	26.73	23.75	28.11

The nature of transition states and intermediates in the catalytic mechanism of glycosidases is a controversial subject due to the complexity of these nucleophilic substitution reactions.[59] Particularly, for TcTS, several aspects of its mechanism have been the subject of discussion. For instance, it has been questioned whether a CI or an oxocarbenium ion is the stable intermediate formed during the course of the reaction which would subsequently react with the target lactose. Yang et al., based on KIE analysis, gave evidence supporting CI formation,[30] and then Tyr342 was proposed as the nucleophile residue.[24] Later, Watts et al. captured a CI using deoxy-2,3-difluorosialic acid as substrate and obtained the X-ray crystal structures.[23] These results together with KIE experiments are highly suggestive that a CI is present during the catalyzed mechanism. Nevertheless, there is still an important mechanistic question to be answered: is the putative carbocation that must occur from the MC to CI an intermediate or a transition state?

Knowledge of the TS for this reaction, for instance, would be very important because it can provide information to design stable analogues as TS inhibitors.[60] Experimentally, the determination of KIEs is the only currently available method that can offer information about this species. Computational studies are a powerful instrument in these scenarios because they can provide a detailed picture of the TS and of the entire mechanistic pathway.

Figure 3a shows the contour plot of the free energy surface that describes the path from the MC toward the CI in the reaction catalyzed by TcTS. The minimum free energy path is highlighted with a white line. For this path, the changes in the distances involved in the reaction coordinate definition are depicted in Figure 3b. As predicted in KIE experimental analysis,[30] results indicate that the most probable pathway corresponds to an A_ND_N mechanism. This type of mechanism was also predicted for other enzymatic *O*- and *N*-glycoside reactions.[61−72] Regarding the energetics, the observed $\Delta G_r^{\#}$ is 20.80 ± 0.7 kcal/mol, and once the TS is reached, the path is downhill toward the CI formation which implies a proton transfer from Tyr342 to Glu230 and a covalent bond formation between Tyr342 and the sialic acid. The computed ΔG_r^0 for the reaction is −0.89 ± 0.43 kcal/mol making the CI roughly equienergetic with the MC. This is a very direct evidence of the formation of this species in the TcTS reaction mechanism. An analogous free energy analysis was recently done on a related enzyme (hen egg white lysozyme) in which the presence of the CI was also predicted, and a similar energy barrier was found.[73] When the 1-D free energy profiles performed at RC1 = 2.5 Å and RC2 = 5.0 Å were compared with the corresponding ones of the 2-D profile to test the convergence of the length of the MD simulation, the differences in $\Delta G_r^{\#}$ and ΔG_r^0 were <1.0 kcal/mol, indicating that the sampling on the 2-D surface was adequate.

In order to better describe the mechanism, a "reaction space" plot, based on a More O'Ferral−Jenk style diagram,[74] is presented in Figure 4. The characteristic parameters of the MC, TS, and CI are presented in Table 2. The commonly used Pauling bond orders[75] of the structures along the minimum free energy path to the leaving group (n_{LG}) and the nucleophile (n_{Nu}) were determined using eq 4:[76]

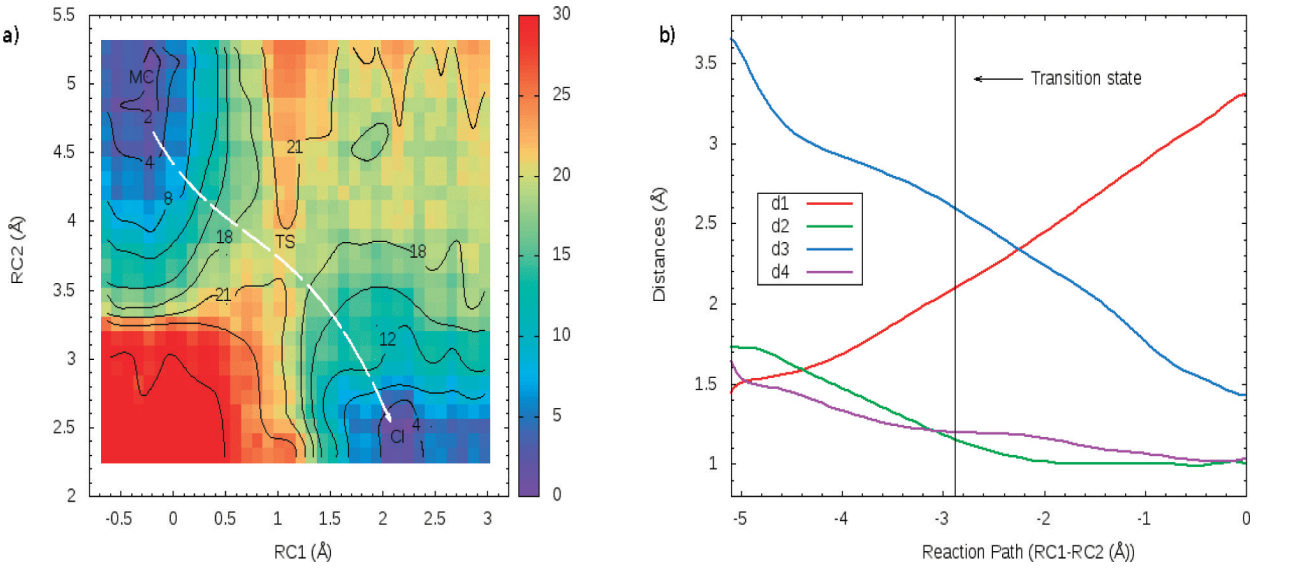

Figure 3. (a) Free energy contour plot of the CI formation in TcTS using sialyllactose as substrate. Results are in kcal/mol. The white line illustrates the minimum free energy path. For this path, the distances involved in the reaction coordinate definition are depicted in (b).

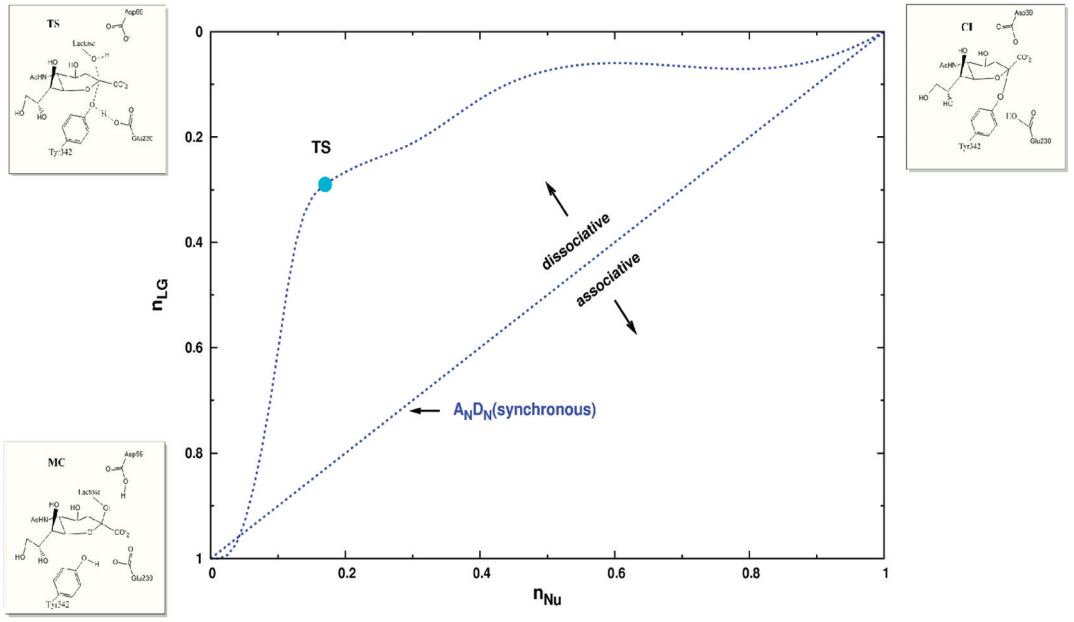

Figure 4. Reaction space for the CI formation in TcTS mechanism. The axes are the Pauling bond orders from the anomeric C to the leaving group (n_{LG}) and the nucleophile (n_{NU}). The reactant, TS, and product configuration are shown in the bottom left, top left, and top right, respectively.

$$N_x = N_0 \exp((R_0 - R_x)/c) \quad (4)$$

where R_x denotes the average distance between the leaving-group/nucleophile and the anomeric C. $N_0 = 1$, $c = 0.6$, and $R_0 = 1.4$ were the values used for the parameters. The reaction path depicted in Figure 4 shows that the leaving group departs well before the TS is reached. This indicates that the A_ND_N mechanism is a dissociative one. The values of $d2$ and $d3$ in Table 2 also show that the Asp59 proton is almost transferred at the TS and that the hydroxyl oxygen of Tyr342 is ~1.0 Å closer to the anomeric C when the TS is reached. In this configuration the hydroxyl oxygen of Tyr342 has become more negative, measured as a (Mulliken) partial charge of −0.47 in the MC and −0.61 at the TS. The enhanced charge would render Tyr342 a better nucleophile. This nucleophilic participation was suggested by Yang et al. on the basis of KIE experiments.[30] Later, it was proposed that Tyr342 was a good choice for the nucleophile because unlike traditional carboxylate nucleophiles, it might have an easier electrostatic approach to the anomeric carbon in the neighborhood of the negatively charged anomeric carboxylate.[23] From KIE experimental results it was also inferred that there was little charge development on the anomeric C when the system goes from the MC to the TS. Table 2 results illustrate that the partial charge of the anomeric C is practically constant during the whole path and that its neighboring O13 (see Figure 2) is instead the atom which suffers a considerable change of its partial charge when the TS is reached. In Figure 5, the anomeric C−O13 distance and the dihedral anomeric C−C10−O13−C19 along the minimum free energy reaction path are

dx.doi.org/10.1021/bi2009618|*Biochemistry* 2011, 50, 10150–10158

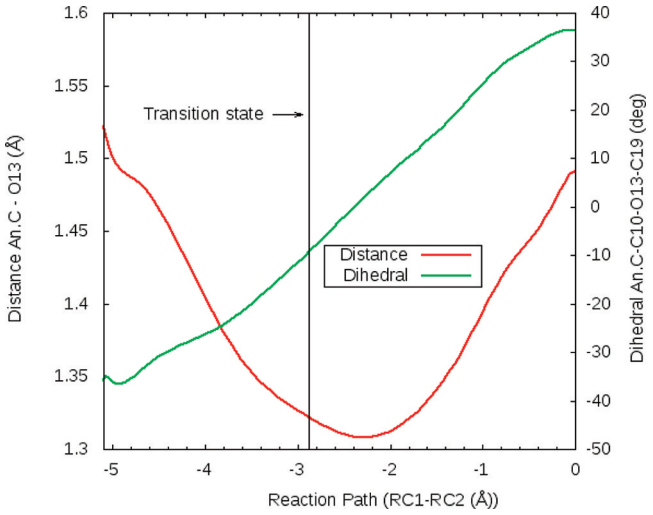

Figure 5. Distance anomeric C−O13 (red) and dihedral angle C9 (anomeric C)−C10−O13−C19 (green) along the minimum free energy path (characterized as RC1−RC2). Atom names correspond to those in the PDB file.

Table 2. Parameters Selected To Illustrate the Characteristics of the MC, TS, and CI[a]

parameter	MC	TS	CI
*d*1	1.512 ± 0.044	2.190 ± 0.042	3.30 ± 0.036
*d*2	1.800 ± 0.046	1.158 ± 0.056	1.023 ± 0.043
*d*3	3.512 ± 0.102	2.524 ± 0.105	1.441 ± 0.026
*d*4	1.580 ± 0.113	1.289 ± 0.089	0.962 ± 0.030
dist (an. C−O13)	1.454 ± 0.035	1.298 ± 0.029	1.485 ± 0.032
OH partial charge	−0.472 ± 0.02	−0.608 ± 0.028	−0.407 ± 0.004
an. C partial charge	0.399 ± 0.006	0.414 ± 0.006	0.4231 ± 0.006
O13 partial charge	−0.414 ± 0.012	−0.182 ± 0.013	−0.4502 ± 0.007

[a]Definitions of *d*1, *d*2, *d*3, and *d*4 are depicted in Figure 2. The values correspond to averages considering the structures sampled on MD simulations related to those configurations. Distances are in Å.

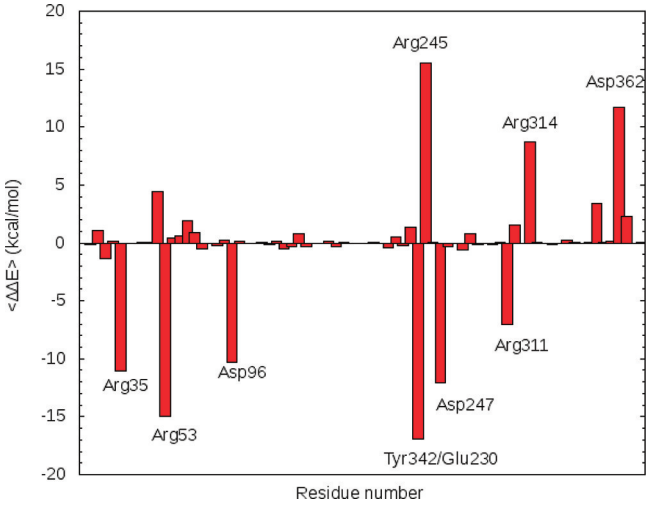

Figure 6. Relative stabilization pattern (eq 2) of the active site residues on the TS considering the MC as reference.

Table 3. Results for β Dideuterium ^{2}H and ^{13}C KIE Calculations Using the B3LYP/6-31G(d) Level of Theory[a]

	sialyllactose acid solvolysis		enzyme reaction	
type of KIE	calcd	exptl	calcd	exptl
β dideuterium ^{2}H	1.161	1.113 ± 0.012	1.065	1.053 ± 0.010
^{13}C primary	1.008	1.016 ± 0.011	1.018	1.021 ± 0.014

[a]Experimental values taken from ref 30 are also shown.

shown. As it can be seen, the anomeric C−O13 bond shortens in going from MC to TS gaining partial double bond character, and at the TS the carbocation is almost planar. Once the CI is reached, the sialic acid ring inverts its configuration and the anomeric C−O13 bond returns to single bond character.

In order to describe the changes in the sialic acid ring during the reaction, we followed IUPAC nomenclature.[77] In the MC, the ring has a $B_{2,5}$ boat conformation. To precisely quantify the puckering coordinates, we calculated the average of the Cremer−Pople parameters[78] over the umbrella coordinates at the relevant states. For the MC configurations, the values for Q, φ, and θ were 0.66 ± 0.05, −14.80 ± 7.52°, and 101.58 ± 5.65°, respectively. The structures sampled at the TS adopt a $^{4}H_{5}$ half-chair conformation where atoms O5, C1, C4, and C5 form the reference plane. In this case the puckering values were Q = 0.54 ± 0.06, φ= −60.12 ± 4.82°, and θ = 148.91 ± 4.01°. Finally, when the CI is reached, the sialic acid ring conformation migrates to a $^{2}C_{5}$ chair considering the same reference plane as for the Michaelis complex. For this chair conformation, the Cremer−Pople parameters obtained were Q = 0.55 ± 0.02, φ= −14.19 ± 11.80°, and θ = 162.94 ± 4.93°.

Most glycoside hydrolases and transferases proceed through highly oxocarbenium ion (carbocation)-like TS, and therefore stabilizing the charged ion is a potential strategy to catalyze the reaction.[79] The energy decomposition method was applied to analyze the stabilization pattern of the active site residues on the TS with respect to the MC. Results are presented in Figure 6. The addition over all the $\Delta\Delta E$ values for each residue represents an indication of the degree of the stabilization of the TS from the enzyme environment on the QM subsystem. The resultant value was −21.09 kcal/mol, indicating a strong stabilizing effect on the TS. Particularly, Asp362 and two arginines (Arg245 and Arg314) out the three of the arginine triad exert a destabilizing effect on the TS. However, this effect does not counteract the stabilizing effect mainly produced by the residues: Arg35, Arg53, Asp96, Glu247, Arg311, and the Glu230−Tyr342 couple. Tyr342−Glu230 is considered as a couple because a proton is transferred from Tyr342 to Glu230, and then the former residues makes a covalent bond with the anomeric C of the sialic acid to reach the CI. The stabilization effect of this couple is large (−16.0 kcal/mol), and it mainly due to the Tyr342 nucleophilic participation in the TS configuration. Arg35 and Asp96 are two residues that directly interact with the substrate and have also a large stabilizing effect on the TS, with their $\Delta\Delta E$ values being −11.0 and −10.3 kcal/mol, respectively. Arg53 forms a hydrogen bond with the carboxylic group of Asp59 which changes its electronic distribution after transferring its proton to the substrate. Lastly, Arg311 interacts with the lactose part of the substrate and Glu247 and, although being close to the active site, does not interact directly with the substrate or with Asp59.

The strict hydrolase *Trypanosoma rangeli sialidase* (TrSA) is an enzyme related to TcTS which, although having a 70%

sequence identity and an overall Cα rmsd of 0.78 Å, possesses only hydrolase activity (i.e., it cannot catalyze the transfer of sialic acid). All stabilizing and destabilizing residues mentioned above are conserved in both TcTS and TrSA. Although, due to a small changes in the relative orientation, there exists the possibility that the stabilization pattern of these residues would not be the same in TrSA and TcTS; it can be inferred that they would produce the same stabilizing effect on the TS structure of the reaction catalyzed by TrSA, and thus, both enzymes would use the same strategy to reach the CI. Besides this, single point mutations in any of the residues that exert a big stabilization effect on the TS would make any of these two enzymes lose their ability to catalyze the reaction.

In Table 3, the results for the estimations and the experimental values of the β dideuterium ^{2}H and ^{13}C KIEs are presented. Regarding the β ^{2}H KIEs, both the estimated and the experimental results indicate that the value for solvolysis is larger than the corresponding value for the enzymatic reaction. Considering the ^{13}C KIEs, B3LYP/6-31G(d) results not only exhibit the same trend that the experimental ones, but also the values are in good agreement. Solvolysis estimations indicate that for this system B3LYP/6-31G(d) frequencies are appropriate to analyze KIEs, being better for the primary ^{13}C case than for secondary β dideuterium ^{2}H one. On the other hand, the correspondence that exists between the computed and the experimental KIE for the enzyme reaction is a clear indication that the TS structure found is appropriate.

CONCLUSIONS

We computed the free energy surface that describes the CI formation in the catalytic mechanism of TcTS with sialyllactose. In accordance with experiments, our results indicate that the most probable path corresponds to a highly dissociative A_ND_N reaction and that there exist a strong nucleophilic participation in the TS and very little charge development at the anomeric C. Although experimental data were suggestive about the formation of the CI for non-fluorinated substrates, our results strongly support this suggestion and provide atomic-level detail for the mechanism. The estimated reaction barrier was 20.8 kcal/mol, and the bond orders at the TS to the leaving group and the nucleophile were 0.26 and 0.16, respectively. The analysis of the Mulliken charges at the TS shows significant charge load for the hydroxyl oxygen of the nucleophile and the O13 atom of the sialic acid. By means of the energy decomposition method, it was determined that the enzyme active site highly stabilizes the TS. Particularly, the couple Tyr342−Glu230, Arg35, Arg53, Glu247, Arg311, and Asp96 are mainly responsible for this effect. ^{13}C and β dideuterium ^{2}H KIEs could also be estimated for a model system calculating the frequencies at the B3LYP 6-31G(d) level of theory, and the results were in accordance with experimental measurements.

Summarizing, even though there are many aspects of this catalyzed reaction that require further clarification, the results presented in this article provide relevant information regarding the mechanistic scenario for the CI formation in TcTS. We hope it can contribute to future studies of this important system and could eventually facilitate development of potent TcTS inhibitors for treatment of Chagas disease.

AUTHOR INFORMATION

Corresponding Author

*Phone: (352) 392-6972. Fax: (352) 392-8722. E-mail: roitberg@ufl.edu.

Funding

This work was funded by the National Institutes of Health (NIH 1R01AI073674-01).

ACKNOWLEDGMENTS

We gratefully acknowledge financial support from National Institutes of Health (NIH 1R01AI073674-01) and supercomputer time granted by Large Allocations Resource Committee (TG-MCA05T010). We also thank Msc. Johan F. Galindo for the corrections and suggestions made after reading this manuscript that helped to improve it.

ABBREVIATIONS

TcTS, *Trypanosoma cruzi trans*-sialidase; MD, molecular dynamics; MM, molecular mechanics; QM, quantum mechanics; WHAM, weighted histogram analysis method; KIE, kinetic isotope effect; MC, Michaelis complex; TS, transition state; CI, covalent intermediate; DFTB, density-functional tight binding; HF, Hartree−Fock; rmsd, root-mean-square deviations; MEP, minimum-energy surface.

REFERENCES

(1) http://www.who.int/TDR.

(2) Yoshida, N., Mortara, R. A., Araguth, M. F., Gonzalez, J. C., and Russo, M. (1989) Metacyclic neutralizing effect of monoclonal antibody 10D8 directed to the 35- and 50-kilodalton surface glycoconjugates of *Trypanosoma cruzi*. *Infect. Immun. 57*, 1663−1667.

(3) Schenkman, S., Eichinger, D., Pereira, M. E. A., and Nussenzweig, V. (1994) Structural and Functional Properties of *Trypanosoma* Trans-Sialidase. *Annu. Rev. Microbiol. 48*, 499−523.

(4) Pereira-Chioccola, V. L., Acosta-Serrano, A., Correia de Almeida, I., Ferguson, M. A., Souto-Padron, T., Rodrigues, M. M., Travassos, L. R., and Schenkman, S. (2000) Mucin-like molecules form a negatively charged coat that protects *Trypanosoma cruzi* trypomastigotes from killing by human anti-alpha-galactosyl antibodies. *J. Cell Sci. 113*, 1299−1307.

(5) Buscaglia, C. A., Campo, V. A., Frasch, A. C., and Di Noia, J. M. (2006) *Trypanosoma cruzi* surface mucins: host-dependent coat diversity. *Nat. Rev. Microbiol. 4*, 229−236.

(6) Pereira, M. E., Zhang, K., Gong, Y., Herrera, E. M., and Ming, M. (1996) Invasive phenotype of *Trypanosoma cruzi* restricted to a population expressing trans-sialidase. *Infect. Immun. 64*, 3884−3892.

(7) Previato, J., Andrade, A. F. B., Pessolani, M. C. V., and Mendonça-Previato, L. (1985) Incorporation of sialic acid into *Trypanosoma cruzi* macromolecules. A proposal for a new metabolic route. *Mol. Biochem. Parasitol. 16*, 85−96.

(8) Schauer, R. (2004) Sialic acids: fascinating sugars in higher animals and man. *Zoology 107*, 49−64.

(9) Varki, A. (1997) Sialic acids as ligands in recognition phenomena. *FASEB J. 11*, 248−255.

(10) Schenkman, R. P., Vandekerckhove, F., and Schenkman, S. (1993) Mammalian cell sialic acid enhances invasion by *Trypanosoma cruzi*. *Infect. Immun. 61*, 898−902.

(11) Schenkman, S., Jiang, M.-S., Hart, G. W., and Nussenzweig, V. (1991) A novel cell surface trans-sialidase of *Trypanosoma cruzi* generates a stage-specific epitope required for invasion of mammalian cells. *Cell 65*, 1117−1125.

(12) Costa, F., Franchin, G., Pereira-Chioccola, V. L., Ribeirão, M., Schenkman, S., and Rodrigues, M. M. (1998) Immunization with a plasmid DNA containing the gene of trans-sialidase reduces *Trypanosoma cruzi* infection in mice. *Vaccine 16*, 768−774.

(13) Pereira-Chioccola, V., Costa, F., Ribeirao, M., Soares, I., Arena, F., Schenkman, S., and Rodrigues, M. (1999) Comparison of antibody and protective immune responses against *Trypanosoma cruzi* infection elicited by immunization with a parasite antigen delivered as naked DNA or recombinant protein. *Parasite Immunol. 21*, 103−110.

(14) Villalta, F., Smith, C. M., Burns, J. M., Chaudhuri, G., and Lima, M. F. (1996) Fab' Fragments of a mAb to a Member of Family 2 of Trans-sialidases of *Trypanosoma cruzi* Block Trypanosome Invasion of Host Cells and Neutralize Infection by Passive Immunizationa. *Ann. N.Y. Acad. Sci. 797*, 242−245.

(15) Belen Carrillo, M., Gao, W., Herrera, M., Alroy, J., Moore, J. B., Beverley, S. M., and Pereira, M. A. (2000) Heterologous Expression of *Trypanosoma cruzi* trans-Sialidase in Leishmania major Enhances Virulence. *Infect. Immun. 68*, 2728−2734.

(16) Mucci, J., Hidalgo, A., Mocetti, E., Argibay, P. F., Leguizamón, M. S., and Campetella, O. (2002) Thymocyte depletion in *Trypanosoma cruzi* infection is mediated by trans-sialidase-induced apoptosis on nurse cells complex. *Proc. Natl. Acad. Sci. U. S. A. 99*, 3896−3901.

(17) El-Sayed, N. M., Myler, P. J., Bartholomeu, D. C., Nilsson, D., Aggarwal, G., Tran, A.-N., Ghedin, E., Worthey, E. A., Delcher, A. L., Blandin, G., Westenberger, S. J., Caler, E., Cerqueira, G. C., Branche, C., Haas, B., Anupama, A., Arner, E., Åslund, L., Attipoe, P., Bontempi, E., Bringaud, F., Burton, P., Cadag, E., Campbell, D. A., Carrington, M., Crabtree, J., Darban, H., da Silveira, J. F., de Jong, P., Edwards, K., Englund, P. T., Fazelina, G., Feldblyum, T., Ferella, M., Frasch, A. C., Gull, K., Horn, D., Hou, L., Huang, Y., Kindlund, E., Klingbeil, M., Kluge, S., Koo, H., Lacerda, D., Levin, M. J., Lorenzi, H., Louie, T., Machado, C. R., McCulloch, R., McKenna, A., Mizuno, Y., Mottram, J. C., Nelson, S., Ochaya, S., Osoegawa, K., Pai, G., Parsons, M., Pentony, M., Pettersson, U., Pop, M., Ramirez, J. L., Rinta, J., Robertson, L., Salzberg, S. L., Sanchez, D. O., Seyler, A., Sharma, R., Shetty, J., Simpson, A. J., Sisk, E., Tammi, M. T., Tarleton, R., Teixeira, S., Van Aken, S., Vogt, C., Ward, P. N., Wickstead, B., Wortman, J., White, O., Fraser, C. M., Stuart, K. D., and Andersson, B. (2005) The Genome Sequence of *Trypanosoma cruzi*, Etiologic Agent of Chagas Disease. *Science 309*, 409−415.

(18) Henrissat, B. (1991) A classification of glycosyl hydrolases based on amino acid sequence similarities. *Biochem. J. 280* (Pt 2), 309−316.

(19) Cantarel, B. L., Coutinho, P. M., Rancurel, C., Bernard, T., Lombard, V., and Henrissat, B. (2009) The Carbohydrate-Active Enzymes database (CAZy): an expert resource for Glycogenomics. *Nucleic Acids Res. 37*, D233−D238.

(20) Sinnott, M. L. (2007) *Carbohydrate Chemistry and Biochemistry*, pp 403−407, The Royal Society of Chemistry, Cambridge.

(21) Amaya, M. F., Watts, A. G., Damager, I., Wehenkel, A., Nguyen, T., Buschiazzo, A., Paris, G., Frasch, A. C., Withers, S. G., and Alzari, P. M. (2004) Structural Insights into the Catalytic Mechanism of *Trypanosoma cruzi* trans-Sialidase. *Structure 12*, 775−784.

(22) Damager, I., Buchini, S., Amaya, M. F., Buschiazzo, A., Alzari, P., Frasch, A. C., Watts, A., and Withers, S. G. (2008) Kinetic and Mechanistic Analysis of *Trypanosoma cruzi* Trans-Sialidase Reveals a Classical Ping-Pong Mechanism with Acid/BaseCatalysis. *Biochemistry 47*, 3507−3512.

(23) Watts, A. G., Damager, I., Amaya, M. L., Buschiazzo, A., Alzari, P., Frasch, A. C., and Withers, S. G. (2003) *Trypanosoma cruzi* Trans-sialidase Operates through a Covalent Sialyl-Enzyme Intermediate:-Tyrosine Is the Catalytic Nucleophile. *J. Am. Chem. Soc. 125*, 7532−7533.

(24) Horenstein, B., Yang, J., and Bruner, M. (2002) Mechanistic variation in the glycosyltransfer of N-acetylneuraminic acid. *Nukleonika 47* (Suppl. 1), S25−S28.

(25) Kirby, A. J. (1987) Mechanism and Stereoelectronic Effects in the Lysozyme Reactio. *Crit. Rev. Biochem. Mol. Biol. 22*, 283−315.

(26) Phillips, D. C. (1967) The hen egg-white lysozyme molecule. *Proc. Natl. Acad. Sci. U. S. A. 57*, 483−495.

(27) Vocadlo, D. J., Davies, G. J., Laine, R., and Withers, S. G. (2001) Catalysis by hen egg-white lysozyme proceeds via a covalent intermediate. *Nature 412*, 835−838.

(28) Bowman, A. L., Grant, I. M., and Mulholland, A. J. (2008) QM/MM simulations predict a covalent intermediate in the hen egg white lysozyme reaction with its natural substrate. *Chem. Commun.*, 4425−4427.

(29) Horenstein, B. A., and Bruner, M. (1996) Acid-Catalyzed Solvolysis of CMP-N-Acetyl Neuraminate: Evidence for a Sialyl Cation with a Finite Lifetime. *J. Am. Chem. Soc. 118*, 10371−10379.

(30) Yang, J., Schenkman, S., and Horenstein, B. A. (2000) Primary ^{13}C and beta-Secondary ^{2}H KIEs for Trans-sialidase. A Snapshot of Nucleophilic Participation during Catalysis. *Biochemistry 39*, 5902−5910.

(31) Buschiazzo, A., Amaya, M. F., Cremona, M. L., Frasch, A. C., and Alzari, P. M. (2002) The Crystal Structure and Mode of Action of Trans-Sialidase, a Key Enzyme in *Trypanosoma cruzi* Pathogenesis. *Mol. Cell 10*, 757−768.

(32) Rye, C. S., and Withers, S. G. (2000) Glycosidase mechanisms. *Curr. Opin. Chem. Biol. 4*, 573−580.

(33) Vasella, A., Davies, G. J., and Böhm, M. (2002) Glycosidase mechanisms. *Curr. Opin. Chem. Biol. 6*, 619−629.

(34) Pierdominici-Sottile, G., and Roitberg, A. E. (2010) Proton Transfer Facilitated by Ligand Binding. An Energetic Analysis of the Catalytic Mechanism of *Trypanosoma cruzi* Trans-Sialidase. *Biochemistry 50*, 836−842.

(35) Guthrie, R. D., and Jencks, W. P. (1989) IUPAC recommendations for the representation of reaction mechanisms. *Acc. Chem. Res. 22*, 343−349.

(36) Case, D. A., Darden, T. A., Cheatham, T. E., III, Simmerling, C. L., Wang, J., Duke, R. E., Luo, R., Crowley, M., Walker., R., Zhang, W., Merz, K. M., Wang, B., Hayik, S., Roitberg, A., Seabra, G., Kolossvary, I., Wong, K. F., Paesani, F., Vanicek, J., Wu, X., Brozell, S. R., Steinbrecher, T., Gohlke, H., Yang, L., T., C., Mongan, J., Hornak, V., Cui, G., Mathews, D. H., Seetin, M. G., Sagui, C., Babin, V., and Kollman, A. P. (2008) University of California, San Francisco.

(37) Jorgensen, W. L., Chandrasekhar, J., Madura, J. D., Impey, R. W., and Klein, M. L. (1983) Comparison of simple potential functions for simulating liquid water. *J. Chem. Phys. 79*, 926−935.

(38) Hornak, V., Abel, R., Okur, A., Strockbine, B., Roitberg, A., and Simmerling, C. (2006) Comparison of multiple Amber force fields and development of improved protein backbone parameters. *Proteins: Struct., Funct., Bioinf. 65*, 712−725.

(39) Cornell, W. D., Cieplak, P., Bayly, C. I., Gould, I. R., Merz, K. M., Ferguson, D. M., Spellmeyer, D. C., Fox, T., Caldwell, J. W., and Kollman, P. A. (1995) A Second Generation Force Field for the Simulation of Proteins, Nucleic Acids, and Organic Molecules. *J. Am. Chem. Soc. 117*, 5179−5197.

(40) Elstner, M., Porezag, D., Jungnickel, G., Elsner, J., Haugk, M., Frauenheim, T., Suhai, S., and Seifert, G. (1998) Self-consistent-charge density-functional tight-binding method for simulations of complex materials properties. *Phys. Rev. B 58*, 7260.

(41) Seabra, G., Walker, R. C., Elstner, M., Case, D. A., and Roitberg, A. E. (2007) Implementation of the SCC-DFTB Method for Hybrid QM/MM Simulations within the Amber Molecular Dynamics Package. *J. Phys. Chem. A 111*, 5655−5664.

(42) Kumar, S., Bouzida, D., Swendsen, R. H., Kollman, P. A., and Rosenberg, J. M. (1992) The weighted histogram analysis method for free-energy calculations on biomolecules. I: The method. *J. Comput. Chem. 13*, 1011−1021.

(43) Torrie, G. M., and Valleau, J. P. (1977) Nonphysical sampling distributions in Monte Carlo free-energy estimation: Umbrella sampling. *J. Comput. Phys. 23*, 187−199.

(44) Chatfield, D. C., P. Eurenius, K., and Brooks, B. R. (1998) HIV-1 protease cleavage mechanism: A theoretical investigation based on classical MD simulation and reaction path calculations using a hybrid QM/MM potential. *J. Mol. Struct.: THEOCHEM 423*, 79−92.

(45) Cunningham, M. A., Ho, L., Nguyen, D. T., Gillilan, R. E., and Bash, P. A. (1997) Simulation of the Enzyme Reaction Mechanism of Malate Dehydrogenase. *Biochemistry 36*, 4800−4816.
(46) Davenport, R. C., Bash, P. A., Seaton, B. A., Karplus, M., Petsko, G. A., and Ringe, D. (1991) Structure of the triosephosphate isomerase-phosphoglycolohydroxamate complex: an analog of the intermediate on the reaction pathway. *Biochemistry 30*, 5821−5826.
(47) Dinner, A. R., Blackburn, G. M., and Karplus, M. (2001) Uracil-DNA glycosylase acts by substrate autocatalysis. *Nature 413*, 752−755.
(48) Garcia-Viloca, M., Truhlar, G., D., and Gao, J. (2003) Reaction-path energetics and kinetics of the hydride transfer reaction catalyzed by dihydrofolate reductase. *Biochemistry 42*, 13558−13575.
(49) Hensen, C., Hermann, C. J., Nam, K., Ma, S., Gao, J., and Holtje, H. (2004) A combined QM/MM approach to protein-ligand interactions: polarization effects of the HIV-1 protease on selected high affinity inhibitors. *J. Med. Chem. 47*, 6673−6680.
(50) Major, D. T., and Gao, J. (2006) A Combined Quantum Mechanical and Molecular Mechanical Study of the Reaction Mechanism and α-Amino Acidity in Alanine Racemase. *J. Am. Chem. Soc. 128*, 16345−16357.
(51) Wong, K.-Y., and Gao, J. (2007) The Reaction Mechanism of Paraoxon Hydrolysis by Phosphotriesterase from Combined QM/MM Simulations. *Biochemistry 46*, 13352−13369.
(52) Frisch, M. J., Trucks, G. W., Schlegel, H. B., Scuseria, G. E., Robb, M. A., Cheeseman, J. R., Scalmani, G., Barone, V., Mennucci, B., Petersson, G. A., Nakatsuji, H., Caricato, M., Li, X., Hratchian, H. P., Izmaylov, A. F., Bloino, J., Zheng, G., Sonnenberg, J. L., Hada, M., Ehara, M., Toyota, K., Fukuda, R., Hasegawa, J., Ishida, M., Nakajima, T., Honda, Y., Kitao, O., Nakai, H., Vreven, T., Montgomery, Jr., J. A., Peralta, J. E., Ogliaro, F., Bearpark, M., Heyd, J. J., Brothers, E., Kudin, K. N., Staroverov, V. N., Kobayashi, R., Normand, J., Raghavachari, K., Rendell, A.; Burant, J. C., Iyengar, S. S., Tomasi, J., Cossi, M., Rega, N., Millam, N. J., Klene, M., Knox, J. E., Cross, J. B.; Bakken, V., Adamo, C.; Jaramillo, J., Gomperts, R., Stratmann, R. E., Yazyev, O., Austin, A. J., Cammi, R., Pomelli, C.; Ochterski, J. W., Martin, R. L., Morokuma, K., Zakrzewski, V. G.; Voth, G. A., Salvador, P., Dannenberg, J. J., Dapprich, S., Daniels, A. D., Farkas, Ö., Foresman, J. B.; Ortiz, J. V.; Cioslowski, J., and Fox, D. J. (2009) *Gaussian 09, Revision. A.02*, Gaussian, Inc., Wallingford, CT.
(53) Miertus, S., Scrocco, E., and Tomasi, J. (1981) Electrostatic interaction of a solute with a continuum. A direct utilizaion of AB initio molecular potentials for the prevision of solvent effects. *Chem. Phys. 55*, 117−129.
(54) Melander, V. L., and Saunders, W. H., Jr. (1980) *Reaction Rates of Isotopic Molecules*, Wiley, New York
(55) Anisimov, V., and Paneth, P. (1999) ISOEFF98. A program for studies of isotope effects using Hessian modifications. *J. Math. Chem. 26*, 75−86.
(56) Kruger, T., Elstner, M., Schiffels, P., and Frauenheim, T. (2005) Validation of the density-functional based tight-binding approximation method for the calculation of reaction energies and other data. *J. Chem. Phys. 122*, 114110−114115.
(57) Woodcock, H. L., Hodošček, M., and Brooks, B. R. (2007) Exploring SCC-DFTB Paths for Mapping QM/MM Reaction Mechanisms. *J. Phys. Chem. A 111*, 5720−5728.
(58) Barnett, C. B., and Naidoo, K. J. (2010) Ring Puckering: A Metric for Evaluating the Accuracy of AM1, PM3, PM3CARB-1, and SCC-DFTB Carbohydrate QM/MM Simulations. *J. Phys. Chem. B 114*, 17142−17154.
(59) Zechel, D. L., and Withers, S. G. (2001) Dissection of nucleophilic and acid-base catalysis in glycosidases. *Curr. Opin. Chem. Biol. 5*, 643−649.
(60) Schramm, V. L. (1999) Enzymatic transition-state analysis and transition-state analogs, in *Methods in Enzymology* (Vern, L., and Schramm, D. L. P., Eds.) pp 301−348, Academic Press, New York.
(61) Berti, P. J., Blanke, S. R., and Schramm, V. L. (1997) Transition State Structure for the Hydrolysis of NAD+ Catalyzed by Diphtheria Toxin. *J. Am. Chem. Soc. 119*, 12079−12088.
(62) Horenstein, B., Parkin, D. W., Estupinan, B., and Schramm, V. L. (1991) Transition-state analysis of nucleoside hydrolase from Crithidia fasciculata. *Biochemistry 30*, 10788−10795.
(63) Huang, X., Tanaka, K. S. E., and Bennet, A. J. (1997) Glucosidase-Catalyzed Hydrolysis of α-d-Glucopyranosyl Pyridinium Salts: Kinetic Evidence for Nucleophilic Involvement at the Glucosidation Transition State. *J. Am. Chem. Soc. 119*, 11147−11154.
(64) Kline, P. C., Rezaee, M., and Lee, T. A. (1999) Determination of Kinetic Isotope Effects for Nucleoside Hydrolases using Gas Chromatography/Mass Spectrometry. *Anal. Biochem. 275*, 6−10.
(65) Kline, P. C., and Schramm, V. L. (1995) Pre-steady-state transition-state analysis of the hydrolytic reaction catalyzed by purine nucleoside phosphorylase. *Biochemistry 34*, 1153−1162.
(66) Lee, J. K., Bain, A. D., and Berti, P. J. (2004) Probing the Transition States of Four Glucoside Hydrolyses with ^{13}C Kinetic Isotope Effects Measured at Natural Abundance by NMR Spectroscopy. *J. Am. Chem. Soc. 126*, 3769−3776.
(67) Mentch, F., Parkin, D. W., and Schramm, V. L. (1987) Transition-state structures for N-glycoside hydrolysis of AMP by acid and by AMP nucleosidase in the presence and absence of allosteric activator. *Biochemistry 26*, 921−930.
(68) Parkin, D. W. (1984) Effects of allosteric activation on the primary and secondary kinetic isotope effects for three AMP nucleosidases. *J. Biol. Chem. 259*, 9418−9425.
(69) Parkin, D. W., Mentch, F., Banks, G. A., Horenstein, B. A., and Schramm, V. L. (1991) Transition-state analysis of a Vmax mutant of AMP nucleosidase by the application of heavy-atom kinetic isotope effects. *Biochemistry 30*, 4586−4594.
(70) Scheuring, J. (1997) Pertussis toxin: transition state analysis for ADP-ribosylation of G-protein peptide alphai3C20. *Biochemistry 36*, 8215−8223.
(71) Scheuring, J. (1998) Transition-state structure for the ADP-ribosylation of recombinant Gialpha1 subunits by pertussis toxin. *Biochemistry 37*, 2748−2758.
(72) Scheuring, J., and Schramm, V. L. (1997) Kinetic Isotope Effect Characterization of the Transition State for Oxidized Nicotinamide Adenine Dinucleotide Hydrolysis by Pertussis Toxin. *Biochemistry 36*, 4526−4534.
(73) Grant, I. M., and Mulholland, A. J. (2008) QM/MM simulations predict a covalent intermediate in the hen egg white lysozyme reaction with its natural substrate. *Chem. Commun.*, 4425−4427.
(74) Jencks, W. P. (1985) A primer for the Bema Hapothle. An empirical approach to the characterization of changing transition-state structures. *Chem. Rev. 85*, 511−527.
(75) Pauling, L. (1947) Atomic Radii and Interatomic Distances in Metals. *J. Am. Chem. Soc. 69*, 542−553.
(76) Houk, K. N., Gustafson, S. M., and Black, K. A. (1992) Theoretical secondary kinetic isotope effects and the interpretation of transition state geometries. 1. The Cope rearrangement. *J. Am. Chem. Soc. 114*, 8565−8572.
(77) IUPAC-IUB Joint Commission on Biochemical Nomenclature (JCBN). (1980) Conformational Nomenclature for Five and Six-Membered Ring Forms of Monosaccharides and Their Derivatives, *Eur. J. Biochem. 111*, 295−298.
(78) Cremer, D., and Pople, J. A. (1975) General definition of ring puckering coordinates. *J. Am. Chem. Soc. 97*, 1354−1358.
(79) Berti, P. J., and McCann, J. A. (2006) Toward a Detailed Understanding of Base Excision Repair Enzymes: Transition State and Mechanistic Analyses of N-Glycoside Hydrolysis and N-Glycoside Transfer. *Chem. Rev. 106*, 506−555.